Int. J. Electrochem. Sci., 9 **(2014)** 2832 - 2847

International Journal of
ELECTROCHEMICAL
SCIENCE
www.electrochemsci.org

Electrodeposition of AuPdCu Alloy Nanoparticles on a Multi-Walled Carbon Nanotube Coated Glassy Carbon Electrode for the Electrocatalytic Oxidation and Determination of Hydrazine

Fang Xu, Lijuan Zhao, Faqiong Zhao[*]*, Lizhi Deng, Ling Hu, Baizhao Zeng*

Key Laboratory of Analytical Chemistry for Biology and Medicine (Ministry of Education), College of Chemistry and Molecular Sciences, Wuhan University, Wuhan 430072, Hubei Province, P. R. China
[*]E-mail: fqzhao@whu.edu.cn

Received: 20 January 2014 / *Accepted:* 2 March 2014 / *Published:* 23 March 2014

AuPdCu nanoparticles were electrodeposited on a multi-walled carbon nanotube (MWCNT) film coated glassy carbon electrode (GCE). The particles were characterized by scanning electron microscope, X-ray diffraction and energy dispersive X-ray spectroscopy. It was found that they were well dispersed on the electrode surface and showed the features of alloy. The AuPdCu nanoparticles presented high electrocatalytic activity to the oxidation of hydrazine, and at the resulting AuPdCu-MWCNT/GCE electrode, hydrazine could produce a sensitive anodic peak in pH 7 phosphate buffer solutions. The peak potential varied with the atomic ratio of Pd/Au in the alloy nanoparticles. Under the optimized conditions, the oxidation current of hydrazine at 0.1 V (vs SCE) was linear to its concentration in the range of 0.1−306 μM (R^2=0.9986) with a sensitivity of 1.26 μA μM^{-1}, and the detection limit was down to 0.02 μM (S/N=3). The electrode also had good reproducibility and selectivity. It was applied to the determination of hydrazine in water samples and the recovery for standards added was 94−101%.

Keywords: AuPdCu nanoparticle; Multi-walled carbon nanotube; Electrodeposition; Hydrazine; Electrochemical sensor; Electrocatalytic oxidation

1. INTRODUCTION

Hydrazine is widely used in agriculture, pharmacy and aerospace etc [1], hence it is unavoidable to be carelessly discharged in the environment. However, hydrazine is an environmental pollutant and it can damage liver and kidney even if people only bring into a little [2, 3]. Therefore, the determination of hydrazine is significant for human health and environmental protection [4].

Hydrazine can be determined by different methods, such as spectrophotometry [5], chemiluminescence [6] and chromatography [7]. It can also be detected by electrochemical method because it has electroactivity. As the electroactivity of hydrazine is weaker at conventional electrodes

(e.g. glassy carbon electrode (GCE), Pt electrode and Au electrode), a number of chemical modified electrodes were prepared and used for such purpose, such as metal nanoparticle modified electrodes [8,9], metal oxide modified electrodes [10], metal complex modified electrodes [11,12], and organic mediator modified electrodes [13,14]. At the modified electrodes, the electrochemical oxidation of hydrazine was promoted and the detection sensitivity was enhanced. Among various modified electrodes, metal nanomaterial modified electrode has attracted increasing attention as it shows high electrocatalysis to hydrazine. For examples, Li et al. reported a sensitive hydrazine sensor based on the electrodeposition of gold nanoparticles on a choline film [15]. Compton et al. fabricated Pd nanoparticles based electrodes for hydrazine detection [16-19], which made the oxidation potential of hydrazine decrease markedly. At the same time, the oxidation current of hydrazine greatly increased.

Alloy nanomaterials generally possess many characters superior to their single-metal components [20, 21], such as higher electrocatalytic activity, catalytic selectivity and physical/chemical stability. Hence, alloy nanomaterials based electrochemical sensors are expected to present better performance. So far a number of alloy nanomaterials have been attempted in fabricating electrochemical sensors and many interesting results are obtained [22-24]. Recently, AuCu alloy nanoparticle was used to prepare hydrazine sensor [25], and the obtained sensor showed enhanced sensitivity and selectivity in comparison with gold nanoparticles modified electrode etc. This encourages us to attempt other alloy nanomaterials in fabricating hydrazine sensors with better property.

In this work, AuPdCu alloy nanoparticles are prepared on a multi-walled carbon nanotube (MWCNT) film coated GCE by electrodeposition and electrochemical oxidation, and the electrochemical behavior of hydrazine is explored. The as-made AuPdCu-MWCNT/GCE shows remarkable catalytic activity, and at the electrode hydrazine can produce a sensitive anodic peak at quite low potential. When it is used for the determination of hydrazine, it presents high sensitivity, selectivity and reproducibility.

2. EXPERIMENTAL

2.1 Reagents and materials

$HAuCl_4$, H_2PdCl_4, $CuSO_4$ and hydrazine were purchased from Sinopharm Chemical Reagent Co. Ltd. (Shanghai, China); MWCNT was from Shenzhen Nanotech Port Co. Ltd. (Shenzhen, China). Hydrazine stock solution (50 mM) was prepared with water and stored in a refrigerator, the working solutions were prepared by diluting the stock solution with 0.1 M phosphate buffer solution (PBS，pH=7.0). All other chemicals used were of analytical reagent grade. The water used was redistilled.

2.2 Apparatus

Electrodeposition, cyclic voltammetric and chronoamperometric experiments were performed with a CHI 660D electrochemical workstation (CH Instrument Company, Shanghai, China). A conventional three-electrode system was adopted. The working electrode was a modified glassy carbon electrode (diameter: 2 mm) or an indium tin oxide slice (ITO, 2 cm×1.5 cm), and the auxiliary and

reference electrodes were a platinum wire and a saturated calomel electrode (SCE), respectively. It should be pointed out here ITO slice was used to perform the scanning electron microscope (SEM) experiment because it could give clearer SEM image than GCE, although they produced very similar SEM images. Energy dispersive X-ray spectra (EDS) and SEM image were obtained using a Hitachi X-650 SEM (Hitachi Co., Japan). X-ray diffraction data were recorded with a Bruke D8 diffractometer (Germany) using Cu Kα radiation (40 kV, 40 mA) with a Ni filter. All measurements were conducted at room temperature.

2.3. Preparation of modified electrodes

Prior to modification, MWCNT was dispersed in redistilled water to prepare 0.5 mg mL^{-1} MWCNT suspension, and the GCE was polished with 0.5 μm alumina slurry and washed with redistilled water. Then 5 μL MWCNT suspension was transferred onto the surface of a GCE and let to dry under an infrared lamp. AuPdCu nanoparticles were electrodeposited on the MWCNT/GCE from the aqueous solution containing 1.5 mM $HAuCl_4$, 0.5 mM $PdCl_2$, 1.0 mM $CuSO_4$ and 0.2 M Na_2SO_4. The electrodeposition potential was set at -0.2 V (vs SCE) and the electrodeposition time was 200 s. The resulting AuPdCu nanoparticles were washed carefully with redistilled water and then dried at room temperature. Thus, an AuPdCu-MWCNT/GCE electrode was conveniently obtained. For comparison, AuCu-MWCNT/GCE, AuPd-MWCNT/GCE, PdCu-MWCNT/GCE, Au-MWCNT/GCE and Pd-MWCNT/GCE electrodes were fabricated through a similar way. Before measurement, the working electrode (e.g. AuPdCu-MWCNT/GCE) was conditioned by repeating the cyclic potential scan between -0.3 V and 1.5 V in a 0.2 M H_2SO_4 solution until a stable cyclic voltammetric curve was obtained. During this process part of Cu and Pd was oxidized and removed.

2.4. Electrochemical measurement procedure

An 8 mL 0.10 M phosphate buffer solution and certain amount of hydrazine stock solution were transferred to a 10 mL cell, and then the three-electrode system was installed on it. Cyclic voltammograms were recorded between -0.6 V − 0.3 V and the chronoamperometric response curves were recorded at 0.10 V.

3. RESULTS AND DISCUSSION

3.1. Morphological analysis

Fig.1 shows the SEM images of ITO, MWCNT/ITO, AuPdCu-MWCNT/ITO and conditioned AuPdCu-MWCNT/ITO. As can be seen, the surface of ITO is quite smooth and MWCNT is discernible. After the electrodeposition of AuPdCu, a lot of nanoparticles are observable. The nanoparticles are quite uniform and well dispersed and their diameters are about 80 nm. After undergoing repetitive cyclic potential scan between -0.3 V and 1.5 V in a 0.2 M H_2SO_4 solution, part of the nanoparticles (e.g. Cu nanoparticles and Pd nanoparticles) and/or part of the metal components

are electrochemically oxidized and removed, and the nanoparticle density decreases to some extent. It should be pointed out when the cyclic voltammetric curve keeps unchanged the remained nanoparticles still contain Cu and Pd as discussed below. This means that the parts of Cu and Pd components in alloy nanoparticles are more stable.

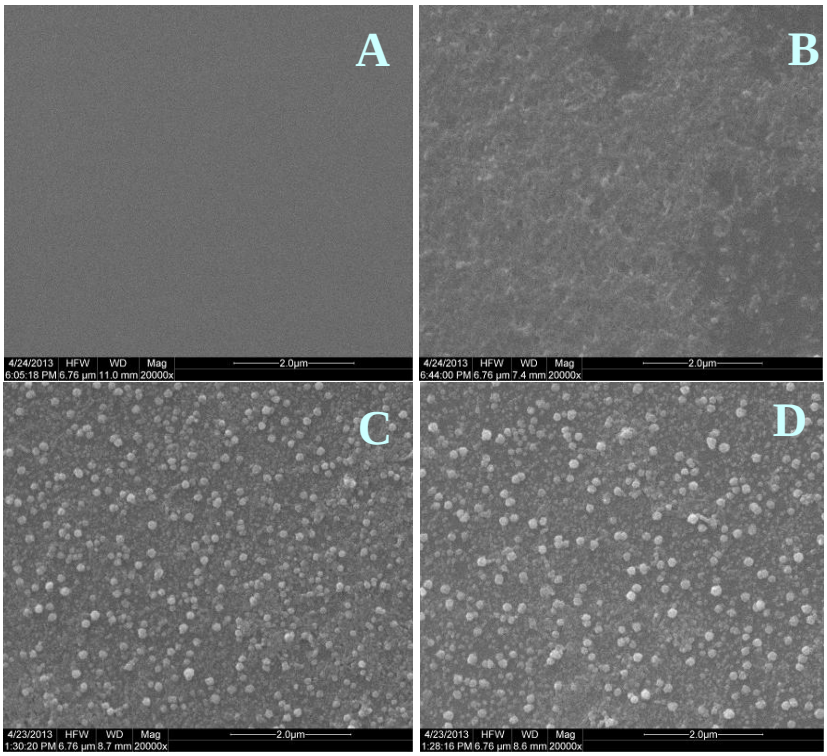

Figure 1. SEM images of ITO (A), MWCNT/ITO (B), AuPdCu-MWCNT/ITO (C) and conditioned AuPdCu-MWCNT/ITO (D). Electrodeposition time: 200 s; deposition potential: -0.2 V (vs SCE); solution composition: 1.5 mM $HAuCl_4$ + 0.5 mM $PdCl_2$ + 1.0 mM $CuSO_4$+0.2 M Na_2SO_4.

3.2. Structure and composition analysis

Fig. 2 shows the XRD patterns of Au, Pd, AuPd and AuPdCu nanoparticles electrodeposited on the MWCNT film coated electrodes. The diffraction patterns display a series of broad Bragg peaks, which are typical for materials of limited structural coherence. The peaks at 38.08°, 44.30°, 64.50° and 77.56° can be assigned to Au (111), (200), (220) and (311) (JCPDS 04-0784), respectively; the peaks at 40.08°, 46.56°, and 68.09° are caused by Pd (111), (200) and (220) (JCPDS 05-0681), respectively. Compared with the corresponding XRD peaks of pure Au nanoparticles and pure Pd nanoparticles, the XRD peaks of AuPdCu nanoparticles lie between them respectively, indicating that the AuPdCu nanoparticles are alloy rather than a mixture of monometallic nanoparticles. The peaks of AuPdCu nanoparticles occur at higher 2θ values than those of AuPd, indicating that the composition and structure of the electrodeposited AuPd nanoparticles is changed in the presence of $CuSO_4$.

The composition of AuPdCu nanoparticles was determined by EDS (Fig. S1). When the concentration ratio of $HAuCl_4$: $PdCl_2$:$CuSO_4$ was 3:1:2 (i. e. 1.5 mM $HAuCl_4$ + 0.5 mM $PdCl_2$ + 1.0

mM $CuSO_4$) the atomic ratio of Au:Pd:Cu in the nanoparticles electrodeposited was 2:1:2. After undergoing repetitive cyclic potential scan between -0.3 V and 1.5 V, the atomic ratio of Au:Pd:Cu in the nanoparticles became 3:1:1. This indicated that part of Pd and part of Cu were removed during the cyclic potential scan. When the concentration ratio of $HAuCl_4$: $PdCl_2$:$CuSO_4$ was changed, the atomic ratio of Au:Pd:Cu in the obtained nanoparticles also changed (Table S1). Therefore, the composition and structure of AuPdCu nanoparticles can be controlled by varying the solution composition.

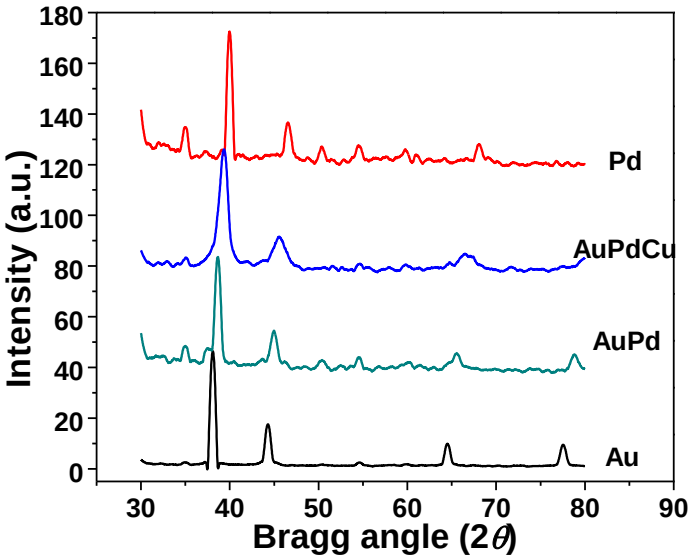

Figure 2. XRD patterns of Au, Pd, AuPd and AuPdCu electrodeposited on MWCNT film (after conditioned). Solution composition for electrodeposition (from top to bottom): 2 mM $PdCl_2$ + 0.2 M Na_2SO_4, 1.5 mM $HAuCl_4$ + 0.5 mM $PdCl_2$ + 1.0 mM $CuSO_4$ + 0.2 M Na_2SO_4, 1.5 mM $HAuCl_4$ + 0.5 mM $PdCl_2$ + 0.2 M Na_2SO_4, 2 mM $HAuCl_4$ + 0.2 M Na_2SO_4. Other conditions as in Fig.1.

3.3. Electrocatalytic oxidation of hydrazine

The cyclic voltammograms of hydrazine at bare GCE, MWCNT/GCE, Au-MWCNT/GCE，Pd-MWCNT/GCE, AuCu-MWCNT/GCE, AuPd-MWCNT/GCE, AuPdCu/GCE and AuPdCu-MWCNT/GCE are displayed in Fig. 3 and Fig. S2. As can be seen, hydrazine does not produce any peaks at bare GCE under this condition. When the GCE is coated by MWCNT, hydrazine exhibits an oxidation peak at about 0.2 V, which can be attributed to the promotion of MWCNT to the electron transfer of hydrazine. However, the peak is broad and the peak current is small. When Au or Pd nanoparticles are electrodeposited on the MWCNT/GCE, the peak potential of hydrazine decreases and the peak current increases. This is due to the catalysis of Au and Pd nanoparticles and the increase in electrode surface area [26-30]. It is clear, at the Pd-MWCNT/GCE, the oxidation peak of hydrazine occurs at quite negative potential (about -0.4 V), but it overlaps with the oxidation peak of Pd, which is unfavorable to the detection of hydrazine. Hydrazine produces a higher oxidation peak at the AuCu-MWCNT/GCE than at the Au-MWCNT/GCE (curves e and f), probably due to the synergic catalysis

of Au and Cu as mentioned in literature [25]. Interestingly, when the AuCu-MWCNT/GCE and Au-MWCNT/GCE is replaced by the AuPd-MWCNT/GCE, the oxidation peak of hydrazine moves from 0 V to -0.2 V (curve h). This means that Pd has some influence on the oxidation potential of hydrazine, unlike Cu. When AuPd nanoparticles are replaced by AuPdCu nanoparticles, the peak current of hydrazine increases further (curve d), while the peak potential keeps almost unchanged. This indicates that Cu element can also cooperate with both Au and Pd in promoting the electrochemical oxidation of hydrazine. Hence, the AuPdCu-MWCNT/GCE electrode is favorable for the detection of hydrazine. It should be pointed out that pure Cu nanoparticles are unstable under these conditions and they are removed during the pretreatment step. Therefore, the increase of peak current cannot be ascribed to the effect of pure Cu nanoparticles. In this case, for comparison, the total concentration of $HAuCl_4$ and $PdCl_2$ is kept unchanged (i.e. *c* ($HAuCl_4$) + *c* ($PdCl_2$) = 2 mM) in the solutions for electrodeposition. In addition, hydrazine produces a much higher oxidation peak at the AuPdCu-MWCNT/GCE than at the AuPdCu/GCE. The reason is that MWCNT has large surface area and it can provide more sites for the formation of AuPdCu nucleus.

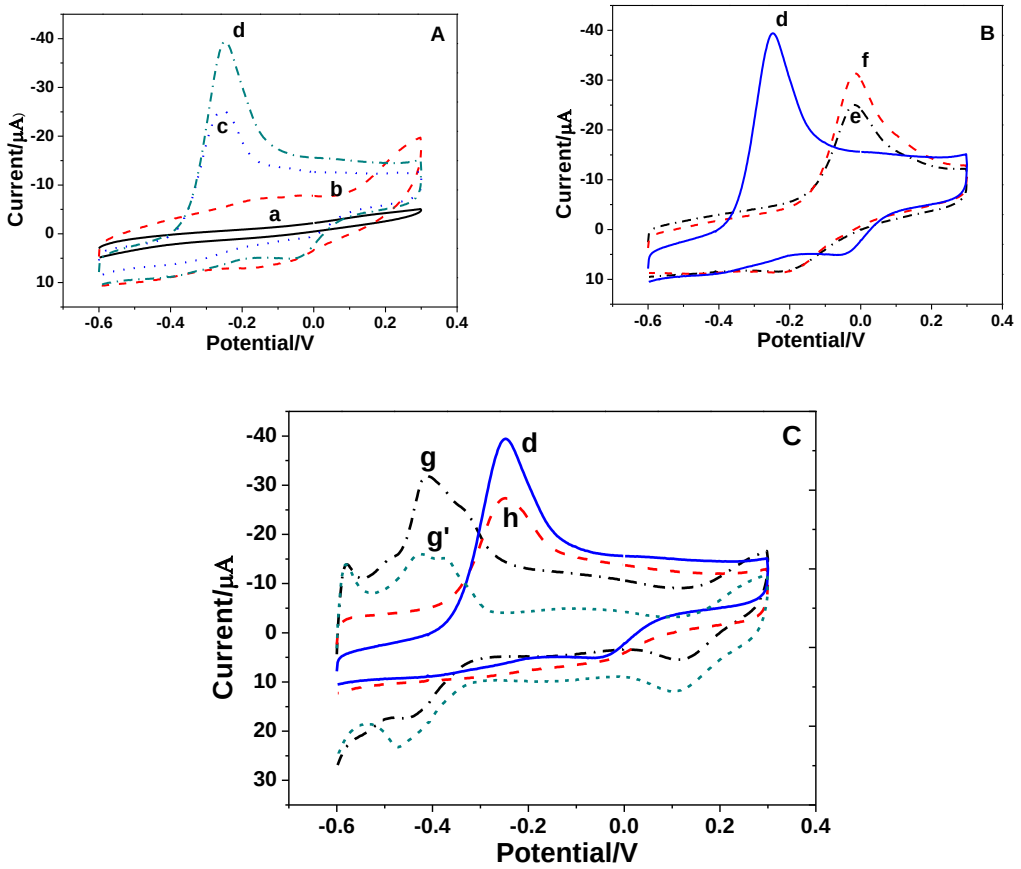

Figure 3. (A) Cyclic voltammograms of bare GCE(a), MWCNT/GCE(b), AuPdCu/GCE (c) and AuPdCu-MWCNT/GCE (d) in 0.1 M PBS containing 0.1 mM hydrazine. (C) Cyclic voltammograms of Au-MWCNT/GCE (e), AuCu-MWCNT/GCE (f), AuPdCu-MWCNT/GCE (d) in 0.1 M PBS containing 0.1 mM hydrazine. (D) Cyclic voltammograms of Pd-MWCNT/GCE (g, g'), AuPd-MWCNT/GCE (h) and AuPdCu-MWCNT/GCE (d) in 0.1 M PBS containing 0.1 mM hydrazine (g) or not (g').

3.4. Effect of the ratio of c ($HAuCl_4$) : c ($PdCl_2$) : c ($CuSO_4$)

As the ratio of *c* ($HAuCl_4$) : *c* ($PdCl_2$) : *c* ($CuSO_4$) affects the composition of AuPdCu nanoparticles electrodeposited (Table S1), the peak current of hydrazine at the resulted AuPdCu-MWNT/GCE is also dependent on it (Fig. S3). Experiments showed when the *c* ($CuSO_4$) was 1 mM and the total concentration of $HAuCl_4$ and $PdCl_2$ was 2 mM, the peak current of hydrazine gradually increased with the ratio of *c* ($HAuCl_4$) : *c* ($PdCl_2$) changing from 7:1 to 3:1. However, when the ratio was further decreased the peak current became small. Therefore, the concentration ratio of $HAuCl_4$ and $PdCl_2$ was kept at 3:1 in the following experiments. The peak current of hydrazine also changed with *c* ($CuSO_4$). When the ratio of *c* ($HAuCl_4$) : *c* ($PdCl_2$) was 3:1 the optimized concentration of $CuSO_4$ was 1 mM. Therefore, an aqueous solution containing 1.5 mM $HAuCl_4$, 0.5 mM $PdCl_2$ and 1 mM $CuSO_4$ was used for electrochemical deposition. In this case, the composition of the alloy nanoparticles electrodeposited was Au_3PdCu, implying that the Au_3PdCu alloy nanoparticles had higher catalytic activity than others, such as AuPdCu and Au_2PdCu. In addition, the peak potential of hydrazine depended on the the ratio of *c* ($HAuCl_4$) : *c* ($PdCl_2$), i.e. the atomic ratio of Au:Pd in alloy nanoparticles. It decreased with increasing the ratio, and lie between the peak potentials of hydrazine at Au-MWCNT/GCE and Pd-MWCNT/GCE. This may be related to the different catalytic activity of different alloy nanoparticles.

3.5. Effect of solution pH

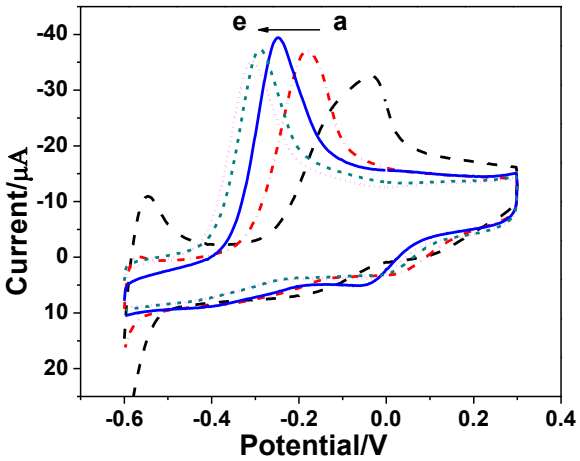

Figure 4. Cyclic voltammograms of AuPdCu-MWCNT/GCE in 0.1 M PBS containing 0.1 mM hydrazine. Solution pH: 5.0 (a), 6.0 (b), 7.0 (c), 7.4 (d), 8.0 (e); scan rate:100 mV/s.

The effect of solution pH on the peak current of hydrazine was investigated over the pH range of 5.0 − 8.0 (Fig. 4). As can be seen, the catalytic peak current increased with pH changing from 5.0 to 7.0, and when the pH was enhanced further, the peak current decreased slightly. This was related to the protonation of hydrazine (pK_a=7.9) and the effect of pH on the catalysis of AuPdCu alloy nanoparticles. It was thought that the protonated hydrazine was not so active [11] and excessive OH^-

may hinder the interaction between hydrazine and AuPdCu alloy. At pH 7.0 the peak current was larger, so pH 7.0 solution was adopted. In addition, with increasing pH the peak potential (E_p) decreased, and the slope of the E_p – pH plot was about 56 mV/pH (Fig. S4). This means that equal numbers of electron and proton were transferred in the electrochemical reaction.

3.6. Effect of electrodeposition potential and electrodeposition time

Electrodeposition potential also showed some influence on the peak current. When the electrodeposition potential was more negative, the electrodeposition of alloy was more rapid and more alloy occurred. But too negative potential led to hydrogen evolution and the aggregation of alloy particles, thus the alloy surface area decreased. In this case, it was found when electrodeposition was performed at -0.2 V, the resulting AuPdCu-MWCNT/GCE exhibited a higher oxidation peak for hydrazine. When electrodeposition was performed at more positive or more negative potential, the peak became smaller (Fig. S5). To extend electrodeposition time more AuPdCu nanoparticles were electrodeposited on the MWCNT/GCE, thus the peak of hydrazine became higher. At about 200 s the peak current reached a maximum value. Then it gradually decreased with further increasing electrodeposition time (Fig. S6). This can be attributed to the aggregation of AuPdCu nanoparticles, which makes the effective electrode area decrease.

3.7. Amperometric measurement of hydrazine

Under the optimized conditions, the chronoamperometric curves of AuPdCu-MWCNT/GCE in hydrazine solutions were recorded (Fig. 5). The electrode showed sensitive response to the change of hydrazine concentration and the response time (reached 95% of the steady-state signal) was several seconds. Furthermore, the response current was linear to hydrazine concentration in the wide range of 0.1 μM − 306 μM (R^2=0.9986), with a sensitivity of 1.26 μA/μM.

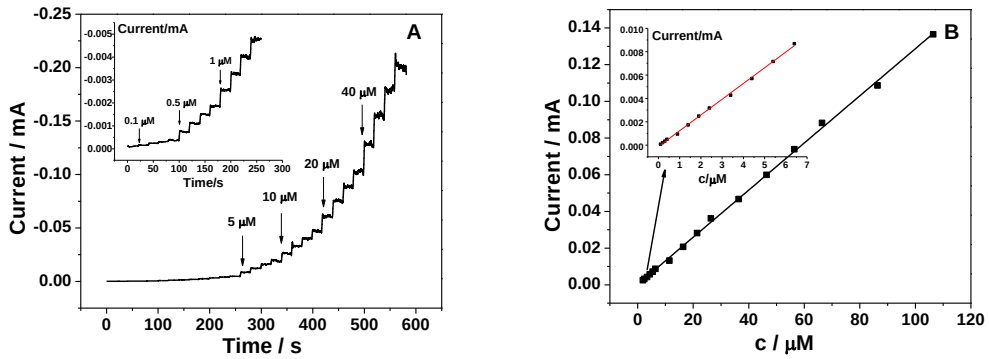

Figure 5. (a) Chronoamperometric response of AuPdCu-MWCNT/GCE to the addition of hydrazine in 0.1 M PBS; (b) the corresponding calibration curve. Solution pH: 7.0; applied potential: 0.10 V. Other conditions as in Fig. 3.

The detection limit was estimated to be 0.02 μM (S/N=3). Compared with other modified electrodes reported for hydrazine the AuPdCu-MWNT/GCE showed acceptable low detection limit and high sensitivity [31-37] (Table S2), although some authors declared a lower detection limit, the sensitivity was lower [35].

3.8. Reproducibility, stability and interference of foreign species

To test the reproducibility and stability of the modified electrode, 20 μM hydrazine was detected with five different electrodes prepared by the same way, and the relative standard deviation (RSD) of the peak current was 5.6%. Twenty successive measurements using one electrode yielded an RSD of 5.2%, indicating that the modified electrode could be used for the repeated detection of hydrazine. The storage stability of the modified electrode was also examined. After one-week store the response current retained 86% of its initial value. After one month it reduced to 78% of the initial value.

The interference of some foreign species for the determination of hydrazine was tested. The results showed that for 40 μM hydrazine K^+, Na^+, Ca^{2+}, Mg^{2+}, Cl^-, SO_4^{2-}, at least 100-fold of NO_3^-, ethanol, methanol, sucrose, glucose and fructose did not interfere with the determination of hydrazine; 5-fold of citric acid, ascorbic acid and uric acid did not present interference (Fig. 6). Therefore, the electrode has some selectivity. This is related to the lower applied potential.

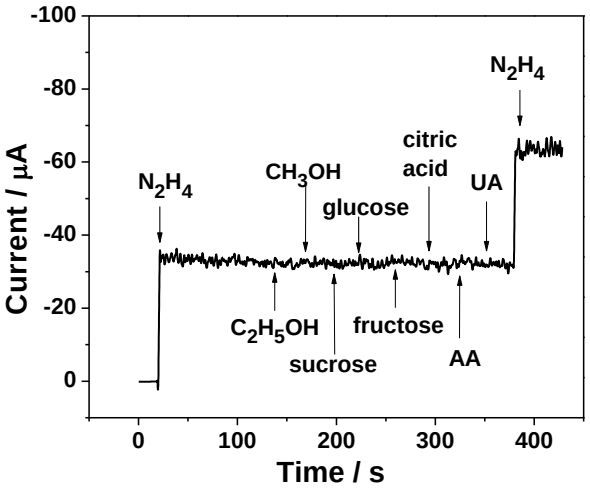

Figure 6. Influence of some coexistents on the response of 40 μM hydrazine. Concentration of ethanol, methanol, sucrose, glucose and fructose: 4 mM; concentration of citric acid, ascorbic acid, uric acid: 0.2 mM; applied potential: 0.1 V.

3.9. Application

The proposed method was applied to the determination of lake water and tap water. But no hydrazine was detected in these samples. Standard hydrazine solutions were then added to the samples to estimate the recovery and the recovery was 94−101% (Table 1).

Table 1. Measurement results of hydrazine in water samples by using the proposed method. (*n*=5)

Samples	Added (μM)	Found (μM)	RSD (%)	Recovery (%)
Tap water	0.0	-	-	-
	50.0	48.1	5.1	96.2
	100.0	94.6	3.2	94.6
Lake water	0.0		-	-
	50.0	48.4	7.7	96.8
	100.0	101.4	4.6	101.4

4. CONCLUSIONS

An AuPdCu alloy nanoparticles-MWCNT composite film modified GCE is fabricated by electrodeposition. The electrode exhibits high electrocatalytic activity to hydrazine oxidation and hydrazine can produce a sensitive anodic peak at quite low potential at it. The electrode shows rapid and sensitive amperometric response to hydrazine and it is suitable for the determination of hydrazine. This work provides a new way to improve the property of electrochemical sensors by utilizing novel alloy nanoparticles.

ACKNOWLEDGEMENTS
The authors appreciate the financial support from the National Natural Science Foundation of China (Grant No.: 21075092).

References

1. A. Umar, M.M. Rahman and Y.B. Hahn, *Talanta*, 77 (2009) 137.
2. S.M. Golabi and H.R. Zare, *J. Electroanal. Chem.*,465 (1999) 168.
3. G. Choudhary and H. Hansen, *Chemosphere*, 37 (1998) 801.
4. A.A. Ensafi and E. Mirmomtaz, *J. Electroanal. Chem.*, 583 (2005) 176.
5. A. Safavi, F. Abbasitabar and M.R.H. Nezhad, *Chem. Anal.*, 52 (2007) 835.
6. A. Safavi and M.A. Karimi, *Talanta*, 58 (2002) 785.
7. J.A. Oh, J.H. Park and H.S. Shin, *Anal. Chim. Acta*, 769 (2013) 79.
8. B. Haghighi, H. Hamidi and S. Bozorgzadeh, *Anal. Bioanal. Chem.*, 398 (2010) 1411.
9. H.J. Zhang, J.S. Huang and H.Q. Hou, T.Y. You, *Electroanal.*, 21 (2009) 1869.
10. B. Dong, B.L. He, J. Huang, G.Y. Gao, Z. Yang and H.L. Li, *J. Power Sources*, 175 (2008) 266.
11. A. Benvidi, P. Kakoolaki, H.R. Zare and R. Vafazadeh, *Electrochim. Acta*, 56 (2011) 2045.
12. M.A. Kamyabi, S. Shahabi and H. Hosseini-Monfared, *J. Electrochem. Soc.*, 155 (2008) 8.
13. S.H. Wu, F.H. Nie, Q.Z. Chen and J.J. Sun, *Anal. Methods*, 2 (2010) 1729.
14. H.M. Nassef, A.E. Radi and C.K. O' Sullivan, *J. Electroanal. Chem.*, 592 (2006) 139.
15. J. Li, H.Q. Xie, L.F. Chen, *Sens. Actuators, B*, 153 (2011) 239.
16. C. Batchelor-McAuley, C.E. Banks, A.O. Simm, T.G.J. Jones and R.G. Compton, *Analyst*, 131 (2006) 106.
17. D.J. Guo and H.L. Li, *Electrochem. Commun.*, 6 (2004) 999.
18. X. Dai, G.G. Wildgoose and R.G. Compton, *Analyst*, 131 (2006) 1241.
19. R. Baron, B. Sljukic, C. Salter and A. Crossley, RG Compton, *Electroanal.*, 19 (2007) 1062.

20. J.A, Rodriquez and D.W. Goodman, *Science*, 260 (1993) 1527.
21. C.Y. Tai, J.L. Chang, J.F. Lee, T.S. Chan and J.M. Zen, *Electrochim. Acta*, 56 (2011) 3115.
22. D.Y. Liu, Q.M. Luo and F.Q. Zhou, *Synthetic Met.*,160 (2010) 1745.
23. M. Tominaga, Y. Taema and I. Taniguchi, *J. Electroanal. Chem.*, 624 (2008) 1.
24. X.L. Yan, F.H. Meng, S.Z. Cui, J.G. Liu, J. Gu and Z.G. Zou, J *J. Electroanal. Chem.*, 661 (2011) 44.
25. L. Shang, F.Q. Zhao and B.Z. Zeng, *Electroanal.*, 24 (2012) 2380.
26. G.H. Chang, Y.L. Luo, W.B. Lu, J.M. Hu, F. Liao and X.P. Sun, *Thin Solid Films*, 519 (2011) 6130.
27. J. Li, H.Q. Xie and L.F. Chen, *Sens. Actuators, B*, 153 (2011) 239.
28. Q.F. Yi and W.Q. Yu, *J. Electroanal. Chem.*, 633 (2009) 159.
29. C.H. Zhang, G.F. Wang, Y.L. Ji, M. Liu, Y.H. Feng, Z.D. Zhang and B. Fang, *Sens. Actuators, B*, 150 (2010) 247.
30. B.K. Jena and C.R. Raj, *J. Phys. Chem. C*, 111 (2007) 6228.
31. Z.J. Yin, L.P. Liu and Z.S. Yang, *J. Solid State Electr.*, 15 (2011) 821.
32. A. Salimi and K. Abdi, *Talanta*, 63 (2004)475.
33. J. Li and X.Q. Lin, *Sens. Actuators, B*, 126(2007) 527.
34. Y. Umasankar, T.Y. Huang and S.M. Chen, *Anal. Biochem.*, 408 (2011) 297.
35. S. Chakraborty and C.R. Raj, *Sens. Actuators, B*, 147 (2010) 222.
36. G.F. Wang, C.H. Zhang, X.P. He, Z.J. Li, X.J. Zhang, L. Wang and B. Fang, *Electrochim. Acta*, 55 (2010) 7204.
37. S. Ivanov, U. Lange, V. Tsakova and V.M. Mirsky, *Sens. Actuators, B*, 150 (2010) 271.

SUPPLEMENTARY DATA:

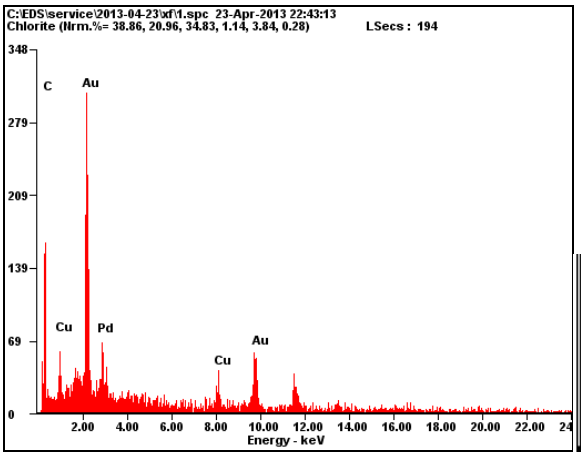

Element	Wt %	At %
C K	63.60	94.76
CuL	07.92	02.23
PdL	05.44	00.92
AuL	23.04	02.09

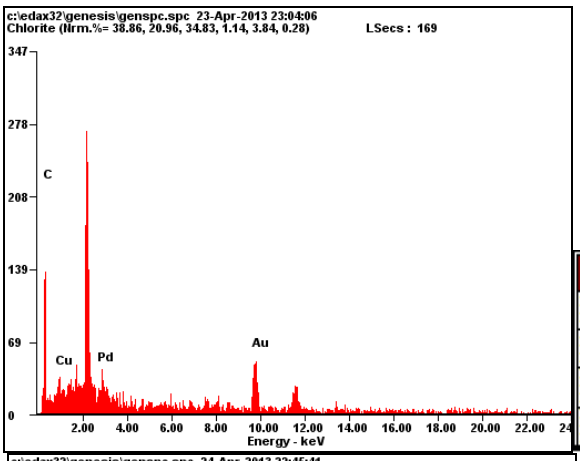

Element	Wt %	At %
C K	61.79	95.42
CuL	02.78	00.81
PdL	05.39	00.94
AuL	30.04	02.83

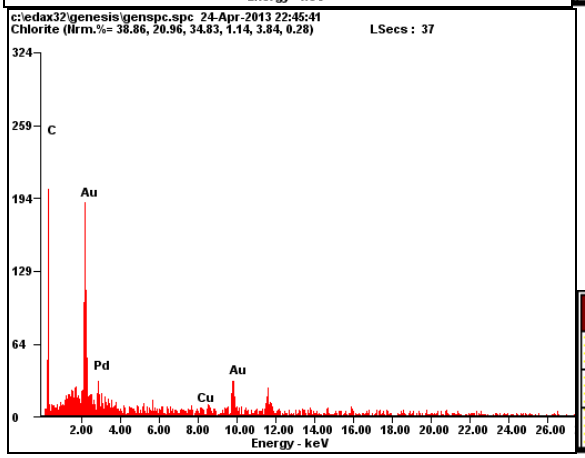

Element	Wt %	At %
C K	74.38	97.63
PdL	03.63	00.54
AuL	21.57	01.73

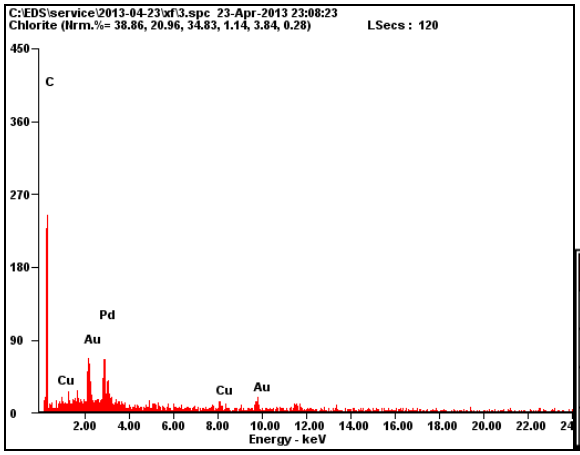

Element	Wt %	At %
C K	81.31	97.74
CuL	03.18	00.72
PdL	06.45	00.88
AuL	09.06	00.66

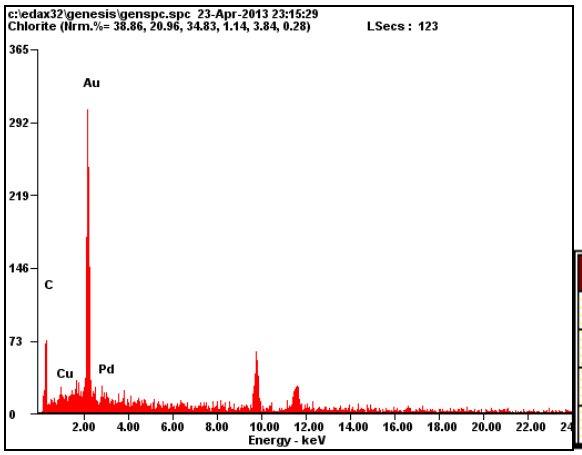

Element	Wt %	At %
C K	43.26	91.08
CuL	04.52	01.80
AuM	48.34	06.21
PdL	03.87	00.92

Figure S1. EDS patterns of different alloy nanoparticles electrodeposited on MWCNT film. The solution for electrodeposition (from top to bottom): 0.2 M Na_2SO_4 + 1.5 mM $HAuCl_4$ + 0.5 mM $PdCl_2$ + 1.0 mM $CuSO_4$, 0.2 M Na_2SO_4 + 1.5 mM $HAuCl_4$ + 0.5 mM $PdCl_2$ + 1.0 mM $CuSO_4$ (after conditioned), 0.2 M Na_2SO_4 + 0.5 mM $HAuCl_4$ + 1.5 mM $PdCl_2$ + 1.0 mM $CuSO_4$, 0.2 M Na_2SO_4 + 1.75 mM $HAuCl_4$ + 0.25 mM $PdCl_2$ + 1.0 mM $CuSO_4$; electrodeposition time: 200 s; deposition potential: -0.2 V (vs SCE).

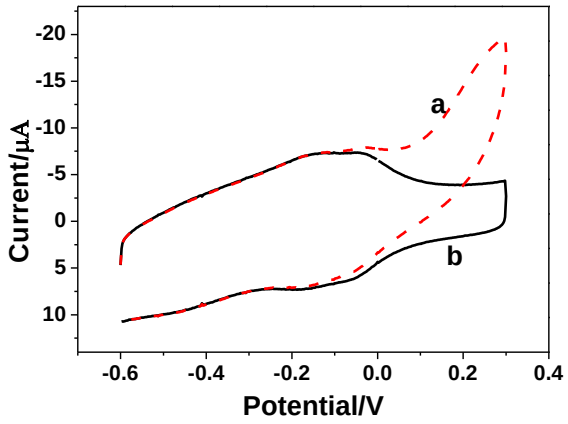

Figure S2. Cyclic voltammograms of MWCNT/GCE in 0.1 M PBS containing 0.1 mM hydrazine (a) or not (b).

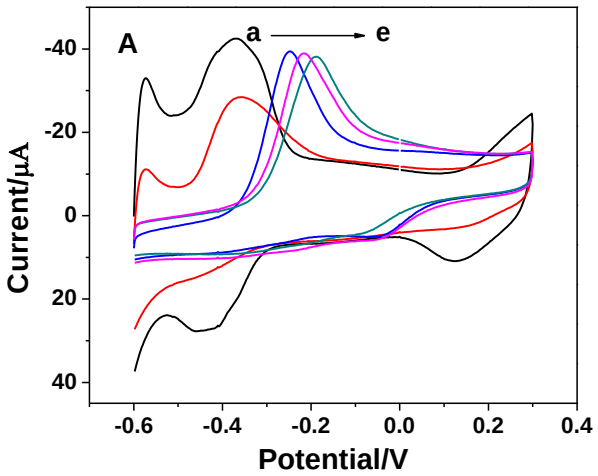

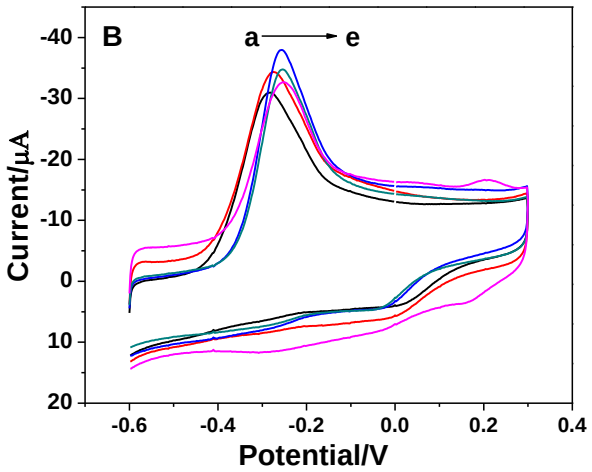

Figure S3. (A) Effect of the ratio of c ($HAuCl_4$) : c ($PdCl_2$) on the anodic peak current of 0.1 mM hydrazine. Concentration of $CuSO_4$: 1 mM; total concentration of $HAuCl_4$ and $PdCl_2$: 2 mM; concentration ratio of $HAuCl_4$ to $PdCl_2$ (a to e): 1:3, 1:1, 3:1, 5:1, 7:1. (B) Effect of $CuSO_4$ concentration on the anodic peak current of 0.1 mM hydrazine. $CuSO_4$ concentration (a to e): 0.25 mM, 0.5 mM, 1.0 mM, 1.5 mM, 2.0 mM; c ($HAuCl_4$): 1.5 mM; c ($PdCl_2$): 0.5 mM. Other conditions as in Fig. 3.

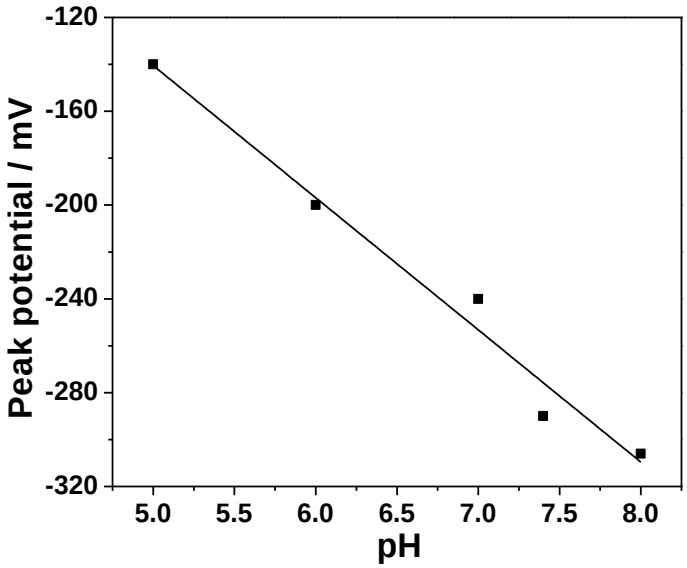

Figure S4. The plot of peak potential vs. pH.

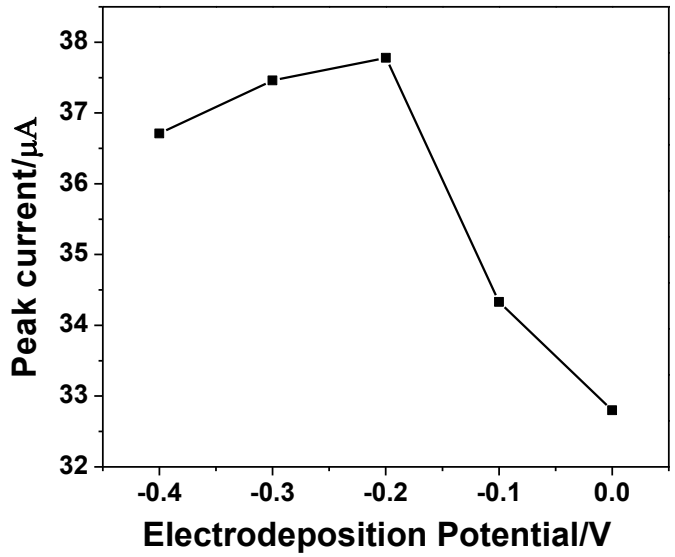

Figure S5. Influence of electrodeposition potential on the peak current of 0.1 mM hydrazine. Electrodeposition potential: 0 V, -0.1 V, -0.2 V, -0.3 V, -0.4 V; the solution composition for electrodeposition: 0.2 M Na_2SO_4 + 1.5 mM $HAuCl_4$ + 0.5 mM $PdCl_2$ + 1.0 mM $CuSO_4$, electrodeposition time: 200 s. Supporting electrolyte: 0.1 M PBS; hydrazine concentration: 0.1 mM.

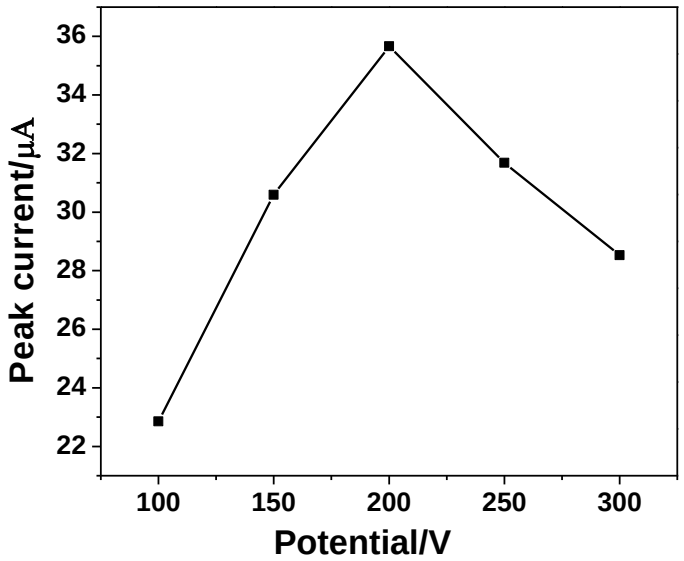

Figure S6. Influence of electrodeposition time on the peak current of 0.1 mM hydrazine. Electrodeposition time: 100 s, 150 s, 200 s, 250 s, 300 s; other conditions as Fig. S3.

Table S1. Dependence of atomic ratio of Au:Pd:Cu in the particles electrodeposited on the concentration ratio of $HAuCl_4$: $PdCl_2$:$CuSO_4$ in electrolyte solutions.

Concentration ratio of $HAuCl_4$: $PdCl_2$:$CuSO_4$ in electrodeposition solution	Atomic ratio of Au:Pd:Cu determined by EDS

(c ($HAuCl_4$) + c ($PdCl_2$) = 2 mM)	*At%*
3:1:2	2:1:2
3:1:2	3:1:1(after conditioned)
3:1:0	3:1:0
7:1:4	6:1:2
1:3:2	3:4:3

Table S2. Comparison of different electrodes for the determination of hydrazine.

Electrodes	LOD (μM)	Sensitivity (μA/μM)	Linear range (μM)	Reference
Nano-copper oxide/GCE	0.03	0.26	0.1−600	[31]
Nickel hexacyanoferrat/carbon composite electrodes	2.28	0.94	2−5000	[32]
Nano-Au/Ppy/GCE[c]	0.2	0.126	1−500	[33]
Au nanoparticles/choline/GCE	0.1	0.0891	0.5−500	[23]
MWCNT-B_{12}/GCE	0.70	1.32	2−1950	[34]
Pt nanoparticles/CNT/GCE	0.0005	0.0195	-	[35]
Nano-Au/Ti electrode	42	1.117	500−4000	[24]
Pd/BDD electrode	1.8	-	10−102	[13]
Nano-Au/porous-TiO_2/GCE	0.5	-	2.5−200	[36]
Pd NPs/polyaniline/GCE	0.06	0.5	10−300	[37]
AuCu-EGN-IL/GCE	0.1	0.056	0.2−110	[25]
AuPdCu-MWCNT/GCE	0.02	1.26	0.1−306	This work